Theory of a two-photon laser amplifier*

Lorenzo M. Narducci and William W. Eidson
Department of Physics and Atmospheric Science, Drexel University, Philadelphia, Pennsylvania 19104

Paul Furcinitti
Department of Biochemistry, Pennsylvania State University, University Park, Pennsylvania 16802

Donald C. Eteson
Electrical Engineering Department, Worcester Polytechnic Institute, Worcester, Massachusetts 01609
(Received 27 January 1977; revised manuscript received 16 June 1977)

We discuss the propagation of an electromagnetic pulse through an active medium prepared in a state of inversion between two levels of the same parity. Since no electric dipole transition is possible between the chosen atomic levels, we investigate the possibility of amplification of an injected signal having a carrier frequency equal to one-half the atomic-transition frequency. We show that under suitable conditions a nonlinear atomic polarization can be generated which oscillates at the same frequency as the incident electromagnetic pulse. The coupled atom-field evolution is described by the usual self-consistent approach. When atomic relaxation effects are negligible, we derive an equation describing the spatial evolution of the energy of the propagating pulse. From this equation we characterize the threshold condition for power amplification and classify the multiple steady-state solutions of the propagation problem. The evolution of the pulse envelope through the amplifier is analyzed with the help of a hybrid computer simulation. Pulse-envelope modulation and multiple-pulse formation even in the asymptotic limit of long amplifiers are displayed.

I. INTRODUCTION

The possibility of producing two-photon stimulated decay and power amplification in a pumped active medium was suggested, apparently for the first time, by Prokhorov[1] and Sorokin and Braslau.[2] Since then, considerable progress has been made in understanding the dynamics of coherent two-photon processes.[3]

Much of the recent work has focused on situations in which the atoms are initially in their ground state; the results have shown surprising qualitative similarities between coherent two-photon processes and their single-photon counterparts[4] (the term coherent is used here, and henceforth, to characterize situations where the atomic relaxation times are much longer than the duration of the propagating pulse). Thus, self-induced transparency, pulse-amplitude and frequency modulation, adiabatic following, and coherent transfer of atomic population have been described theoretically.[5] Experiments on coherent two-photon processes have also been reported.[6]

More limited attention has been directed to the propagation of a pulse in an inverted medium when the active levels are not coupled by a direct electric dipole transition.[7,8] Past experience with one-photon processes has shown that rather minor formal differences exist between the working equations for an amplifying medium[9] and those which are appropriate for an absorbing system.[10] This is still true in the theoretical analysis of atoms undergoing two-photon emission or absorption. However, the theory of a two-photon amplifier predicts interesting effects which have no analog if the atoms are initially unexcited. Thus, for example, we find that, while a two-photon absorber allows the propagation of a Lorentzian-shaped steady-state pulse, the coherent two-photon amplifier cannot support a steady-state-pulse envelope. On the other hand, the pulse energy satisfies an equation that allows different classes of steady-state solutions.

In this paper, we discuss the theory of a degenerate two-photon amplifier. The term degenerate indicates that the carrier frequency of the incident pulse is approximately one-half of the atomic transition frequency. We require the incident pulse to satisfy the slowly varying envelope and phase approximation, and in addition we restrict our attention to pulse durations which are sufficiently smaller than the atomic incoherent relaxation times.

Our analysis evolves along the lines mapped out by Estes *et al.*[7] We describe in some detail the derivation of the coupled atom-field equations of motion and construct an equation for the pulse energy which is reminiscent of the well-known Arecchi-Bonifacio "area equation" for a one-photon amplifier. In this case, however, we discover a much richer variety of solutions that include single as well as multiple pulses. In addition, our energy

equation is integrable and leads to explicit predictions regarding the asymptotic (large-distance) behavior of the pulse energy. The threshold condition for power amplification requires simultaneously an appropriate population inversion between the active levels and a sufficiently large input energy. As a result, small-signal amplification cannot be supported by a two-photon amplifier. On the other hand, if the power amplification conditions are met, a propagating pulse undergoes envelope modulation leading to pulse sharpening and, under appropriate conditions, multiple-pulse formation.

II. BLOCH EQUATIONS FOR THE ACTIVE MEDIUM

We formulate our calculations for a typical atomic system with an energy-level diagram such as shown in Fig. 1. The levels labeled $|a\rangle$ and $|b\rangle$ are assumed to have identical parity, while the intermediate states, labeled $|j\rangle$, are coupled to either $|a\rangle$ or $|b\rangle$ (or both) by a direct dipole transition.

The total Hamiltonian of the system has the form

$$H = E_a|a\rangle\langle a| + E_b|b\rangle\langle b| + \sum_j E_j|j\rangle\langle j| - \vec{p}\cdot\vec{\mathcal{E}}(x,t), \tag{2.1}$$

where the electric field $\vec{\mathcal{E}}(x,t)$ has the familiar form of a propagating plane wave with a slowly varying envelope and phase

$$\vec{\mathcal{E}}(x,t) = \vec{\mathcal{E}}_0(x,t)\cos[\omega t - kx + \varphi(x,t)]. \tag{2.2}$$

The carrier frequency ω is approximately equal to one-half the atomic transition frequency $\omega_{ba} = (E_b - E_a)/\hbar$. We classify this situation as degenerate to distinguish it from the more general case in which two fields of different frequencies, ω_1 and ω_2 ($\omega_1 + \omega_2 = \omega_{ba}$), are propagated through the medium. The dipole-moment operator is assumed to have the form

$$\vec{p} = \sum_j |a\rangle\langle j|\vec{p}_{aj} + |b\rangle\langle j|\vec{p}_{aj} + (\text{hermitian adjoint}). \tag{2.3}$$

The coupling terms between intermediate states, i.e., terms of the form $|j\rangle\langle j'|\vec{p}_{jj'}$, are neglected in Eq. (2.3) since, under the present conditions, the atomic population is expected to be distributed only between the two active levels $|a\rangle$ and $|b\rangle$.

Our calculation is based on the traditional self-consistent approach. We construct equations of motion for the relevant atomic amplitudes C_a and C_b driven by the applied electric field. We then derive an expression for the atomic polarization in terms of the atomic amplitudes, and require, self-consistently, that the polarization act as a source term for the classical field-propagation equations. This approach was adopted to the description of a one-photon amplifier by Arecchi and Bonifacio.[9] Their results will be recalled in our discussion to emphasize the similarities and the differences between the one- and two-photon amplifier theories.

Our starting point is the Schrödinger equation,

$$i\hbar\frac{\partial}{\partial t}|\psi(t)\rangle = H|\psi(t)\rangle, \tag{2.4}$$

for a typical atom described by a state vector

$$|\psi(t)\rangle = \sum_j C_j(t)e^{-iE_jt/\hbar}|j\rangle + C_a(t)e^{-iE_at/\hbar}|a\rangle + C_b(t)e^{iE_bt/\hbar}|b\rangle. \tag{2.5}$$

The atomic state vector evolves under the action of the total Hamiltonian given by Eqs. (2.2) and (2.3). The atomic amplitudes C_j, C_a, C_b are assumed to be slowly varying in time, i.e., to reflect only the secular variations of the state vector. This assumption is well justified for single-photon processes under resonance conditions. In this case, in addition to requiring that $\omega \approx \frac{1}{2}\omega_{ba}$, we must neglect competing radiative processes which cause the atom to radiate at a different frequency from that of the stimulating field. In the presence of a strong signal at frequency ω this assumption appears justified.

The exact coupled equations for the atomic amplitudes are

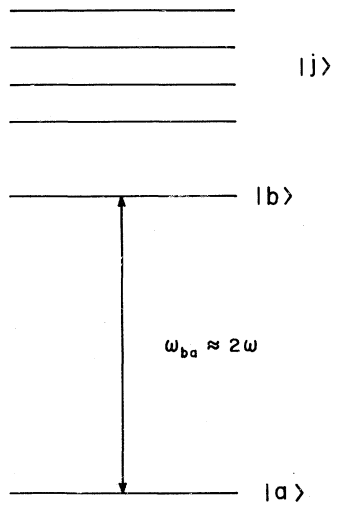

FIG. 1. Schematic energy-level diagram for an active atom. The energy separation between the states $|a\rangle$ and $|b\rangle$ is approximately twice the energy of an incident photon. The symbol $|j\rangle$ collectively represents all the intermediate states.

$$
\begin{aligned}
i\hbar\dot{C}_a(t) &= -\sum_j \mu_{aj}\mathcal{E}(x,t)C_j(t)e^{-i\omega_{ja}t},\\
i\hbar\dot{C}_b(t) &= -\sum_j \mu_{bj}\mathcal{E}(x,t)C_j(t)e^{-i\omega_{jb}t},\\
i\hbar\dot{C}_j(t) &= -\mu_{ja}\mathcal{E}(x,t)C_a(t)e^{i\omega_{ja}t}\\
&\quad -\mu_{jb}\mathcal{E}(x,t)C_b(t)e^{i\omega_{jb}t},
\end{aligned}
\tag{2.6}
$$

where we have assumed the field to be linearly polarized and where the dipole matrix elements μ_{ja} and μ_{jb} are projections along the direction of polarization of the field.

Our objective is to derive a set of coupled equations for the coherent amplitudes C_a and C_b. To this purpose we solve formally for the intermediate amplitudes $C_j(t)$ and replace Eqs. (2.6) by a pair of coupled integrodifferential equations for $C_a(t)$ and $C_b(t)$. The result is

$$
\begin{aligned}
i\hbar\dot{C}_a(t) = -\sum_j \mu_{aj}\mathcal{E}(x,t)e^{-i\omega_{ja}t}\\
\times\frac{i}{\hbar}\int_0^t dt'[\mu_{ja}\mathcal{E}(x,t')C_a(t')e^{i\omega_{ja}t'}\\
+\mu_{jb}\mathcal{E}(x,t')C_b(t')e^{i\omega_{jb}t'}].
\end{aligned}
\tag{2.7}
$$

A similar equation for $C_b(t)$ can be obtained from Eq. (2.7) by interchanging the indices a and b with one another. In order to reduce the exact integrodifferential equations to a manageable form, we perform the slowly varying amplitude approximation for both the atomic amplitudes and for the field envelope. This amounts to replacing $\mathcal{E}_0(x,t')$, $C_a(t')$, and $C_b(t')$ inside the integral with their values at the upper limit of integration, and carrying out the exact integration of the remaining exponential factors.

Upon retaining only the slowly varying terms, the required coupled equations for the atomic amplitudes $C_a(t)$ and $C_b(t)$ take the form

$$
\begin{aligned}
\dot{C}_a(t) &= (i/\hbar)[k_{aa}|E_0|^2C_a(t) + k_{ab}E_0^2C_b(t)e^{i(2\omega-\omega_{ba})t}],\\
\dot{C}_b(t) &= (i/\hbar)[k_{bb}|E_0|^2C_b(t) + k_{ab}E_0^{*2}C_a(t)e^{-i(2\omega-\omega_{ba})t}],
\end{aligned}
\tag{2.8}
$$

where the parameters k_{aa}, k_{bb}, and k_{ab} are given by

$$
\begin{aligned}
k_{aa} &= \frac{2}{\hbar}\sum_j \mu_{ja}^2\frac{\omega_{ja}}{\omega_{ja}^2-\omega^2},\\
k_{bb} &= \frac{2}{\hbar}\sum_j \mu_{jb}^2\frac{\omega_{jb}}{\omega_{jb}^2-\omega^2},\\
k_{ab} &= \frac{1}{\hbar}\sum_j \frac{\mu_{ja}\mu_{jb}}{\omega_{jb}+\omega},
\end{aligned}
\tag{2.9}
$$

and where the slowly time-varying field amplitude E_0 is defined by

$$
\begin{aligned}
\mathcal{E}(x,t) &= \mathcal{E}_0(x,t)\cos[\omega t - kx + \varphi(x,t)]\\
&= E_0(x,t)e^{i\omega t} + E_0^*(x,t)e^{-i\omega t},\\
E_0(x,t) &= \tfrac{1}{2}\mathcal{E}_0(x,t)e^{-i(kx-\varphi)}.
\end{aligned}
\tag{2.10}
$$

As an internal consistency check of the elimination of the intermediate amplitudes, we observe that

$$
\frac{d}{dt}(|C_a|^2 + |C_b|^2) = 0 \tag{2.11}
$$

as one must expect from probability-conservation requirements.

Within the approximations leading to the system of Eq. (2.8), we have replaced the exact dynamical evolution of the multilevel atom with a description that bears considerable similarity to the traditional analysis of a two-level system. The major difference, of course, is that Eqs. (2.8) contain the square of the field envelope, rather than the first power of the field as in the usual description of one-photon processes in a two-level system.

Next, we derive an expression for the atomic polarization in terms of the relevant amplitudes C_a and C_b. From the definition

$$
P = N\langle p\rangle = N\langle\psi(t)|p|\psi(t)\rangle \tag{2.12}
$$

and the operator representation (2.3) for the atomic dipole moment we find, as expected, that the total polarization depends on the entire set of atomic amplitudes, i.e.,

$$
P = N\left(\sum_j \mu_{ja}C_aC_j^*e^{i\omega_{ja}t} + \sum_j \mu_{jb}C_bC_j^*e^{i\omega_{jb}t} + \text{c.c}\right). \tag{2.13}
$$

The elimination of the intermediate amplitudes $C_j(t)$ is carried out in identical fashion as in the derivation of the equations of motion (2.8). Thus, we replace $C_j(t)$ with their formal solution in terms of $C_a(t)$ and $C_b(t)$ and carry out the time integration after making the slowly-varying-amplitude approximation. The result of this calculation reveals polarization terms which oscillate at frequency ω, as well as terms oscillating at frequencies ω_{ja}, ω_{jb}, and at the third harmonic of the incident frequency. Thus, as already remarked (Grischkowsky *et al.* in Ref 5), competing effects may accompany two-photon emission or absorption processes.

In the presence of an injected field at frequency ω, it appears reasonable to ignore all the polarization contributions other than those which oscillate at the frequency of the externally injected pulse. In this case, the atomic polarization takes the form

$$P = N[k_{aa}|C_a|^2 + k_{bb}|C_b|^2 + k_{ab}(C_aC_b^*e^{-i\alpha} + C_a^*C_be^{i\alpha})]\mathcal{E}_0(x,t)\cos[\omega t - kx + \varphi(x,t)]$$
$$+ Nk_{ab}i(C_aC_b^*e^{-i\alpha} - C_a^*C_be^{i\alpha})\mathcal{E}_0(x,t)\sin[\omega t - kx + \varphi(x,t)], \tag{2.14}$$

where

$$\alpha = (2\omega - \omega_{ba})t - 2kx + 2\varphi(x,t). \tag{2.15}$$

It is apparent from Eq. (2.14) that, as in the one-photon case, the induced atomic polarization contains terms that oscillate in-phase and terms that oscillate in quadrature with the applied field. The in-phase component of the polarization in Eq. (2.14), however, depends not only on bilinear terms of the type $C_aC_b^*$, but also on the populations of the active levels through C_a^2 and C_b^2.

By analogy with the Bloch-vector representation of the one-photon theory, it is convenient to introduce the new atomic variables

$$R_1 = i(C_a^*C_be^{i\alpha} - C_aC_b^*e^{-i\alpha}),$$
$$R_2 = -(C_aC_b^*e^{-i\alpha} + C_a^*C_be^{i\alpha}), \tag{2.16}$$
$$R_3 = |C_b|^2 - |C_a|^2.$$

The physical meaning of R_3 and R_1 is immediately obvious: R_3 represents the population difference between the two levels of interest, while R_1 is proportional to the quadrature component of the nonlinear polarization. R_2, however, is no longer proportional to the in-phase component of the polarization because of the dependence of $P(x,t)$ on the atomic populations.

In terms of the new variables, the atomic evolution is described by the set of equations

$$\dot{R}_1 = \left[\frac{k_{bb}-k_{aa}}{4\hbar}\mathcal{E}_0^2 + \left(2\omega - \omega_{ba} + 2\frac{\partial\varphi}{\partial t}\right)\right]R_2 + \frac{k_{ab}}{2\hbar}\mathcal{E}_0^2R_3,$$
$$\dot{R}_2 = -\left[\frac{k_{bb}-k_{aa}}{4\hbar}\mathcal{E}_0^2 + \left(2\omega - \omega_{ba} + 2\frac{\partial\varphi}{\partial t}\right)\right]R_1, \tag{2.17}$$
$$\dot{R}_3 = -\frac{k_{ab}}{2\hbar}\mathcal{E}_0^2R_1,$$

while the atomic polarization takes the form

$$P = -Nk_{ab}\mathcal{E}_0\left[R_2 - \frac{k_{bb}-k_{aa}}{2k_{ab}}\left(R_3 + \frac{k_{aa}+k_{bb}}{k_{bb}-k_{aa}}\right)\right]$$
$$\times\cos(\omega t - kx + \varphi) - Nk_{ab}\mathcal{E}_0R_1\sin(\omega t - kx + \varphi). \tag{2.18}$$

The conservation probability (2.11) is mapped into the conservation of the length of the Bloch vector

$$\frac{d}{dt}(R_1^2 + R_2^2 + R_3^2) = 0 \tag{2.19}$$

which follows at once from Eqs. (2.17).

On comparing Eqs. (2.17) with the usual Bloch equations for a two-level system we note two major differences: in Eqs. (2.17) the atomic variables are driven by the square of the electric field envelope, rather than by the field envelope itself, and the detuning variable contains an intensity-dependent contribution. The immediate consequence of the latter feature is that, even in resonance ($2\omega = \omega_{ba}$ and $\partial\varphi/\partial t = 0$), the second component R_2 of the Bloch vector does not vanish for all time. This factor will be shown explicitly and discussed in Sec. III.

III. COUPLED SCHRÖDINGER-MAXWELL EQUATIONS

The field evolution is described by the wave equation

$$\frac{\partial^2}{\partial x^2}\mathcal{E} - \frac{1}{c^2}\frac{\partial^2\mathcal{E}}{\partial t^2} = \frac{1}{c^2\epsilon_0}\frac{\partial^2P}{\partial t^2}. \tag{3.1}$$

In the slowly varying envelope and phase approximation Eq. (3.1) is equivalent to

$$\mathcal{E}_0\left(c\frac{\partial}{\partial x} + \frac{\partial}{\partial t}\right)\varphi = -\frac{\omega}{2\epsilon_0}P_c, \tag{3.2}$$

$$c\left(\frac{\partial}{\partial x} + \frac{\partial}{\partial t}\right)\mathcal{E}_0 = -\frac{\omega}{2\epsilon_0}P_s, \tag{3.3}$$

where P_c and P_s are the in-phase and in-quadrature components of the polarization in Eq. (2.18). In terms of the atomic variables, the field equations (3.2) and (3.3) can be cast into the form

$$\left(c\frac{\partial}{\partial x} + \frac{\partial}{\partial t}\right)\left(2\omega - \omega_{ba} + 2\frac{\partial\varphi}{\partial t}\right)$$
$$= \frac{\omega Nk_{ab}}{\epsilon_0}\left(\dot{R}_2 - \frac{k_{bb}-k_{aa}}{2k_{ab}}\dot{R}_3\right), \tag{3.4}$$

$$\left(c\frac{\partial}{\partial x} + \frac{\partial}{\partial t}\right)\mathcal{E}_0^2 = \frac{\omega Nk_{ab}}{\epsilon_0}R_1\mathcal{E}_0^2. \tag{3.5}$$

The coupled set of equations (2.17), (3.4), and (3.5) represent the starting point of our analysis.

It is convenient to introduce the following notations

$$\gamma = (k_{bb}-k_{aa})/2k_{ab}, \quad g = \omega Nk_{ab}/\epsilon_0,$$
$$\omega_R = (1+\gamma^2)^{1/2}(k_{ab}/2\hbar)\mathcal{E}_0^2, \tag{3.6}$$
$$\Omega = (2\omega - \omega_{ba}) + 2\frac{\partial\varphi}{\partial t},$$

and to refer the atom-field evolution to the local coordinate frame

$$\eta = x/c, \quad \tau = t - x/c. \tag{3.7}$$

The coupled Schrödinger-Maxwell equations can be written in the form

$$\frac{\partial R_1}{\partial t} = \left(\frac{\gamma}{(1+\gamma^2)^{1/2}}\omega_R + \Omega\right)R_2 + \frac{\omega_R}{(1+\gamma^2)^{1/2}}R_3 ,$$

$$\frac{\partial R_2}{\partial t} = -\left(\frac{\gamma}{(1+\gamma^2)^{1/2}}\omega_R + \Omega\right)R_1 , \tag{3.8}$$

$$\frac{\partial R_3}{\partial t} = -\frac{\omega_R}{(1+\gamma^2)^{1/2}} ;$$

$$\frac{\partial \omega_R}{\partial \eta} = g\omega_R R_1 - l\omega_R , \tag{3.9}$$

$$\frac{\partial \Omega}{\partial \eta} = g\left(\frac{\partial R_2}{\partial \tau} - j\frac{\partial R_3}{\partial \tau}\right) .$$

The field-envelope equation is written in terms of the "Rabi frequency" ω_R which is proportional to the square of the field envelope. The damping term $-l\omega_R$ has been added phenomenologically to describe the effects of nonresonant losses.

In the coherent propagation limit, i.e., neglecting atomic relaxation effects, the field equation can be cast into the form

$$\frac{\partial \omega_r}{\partial t} = g\omega_r R_1 - l\omega_r ,$$

$$\frac{\partial \Omega}{\partial \eta} = -g\Omega R_1 , \tag{3.10}$$

which reveal an interesting conservation relation for the product of the Rabi frequency ω_R and the detuning Ω. In fact, from Eqs. (3.10), we find

$$\frac{\partial}{\partial \eta}(\omega_R\Omega) = -l\omega_R\Omega . \tag{3.11}$$

Equation (3.11) can be integrated at once to yield

$$(\omega_R\Omega)_\eta = (\omega_R\Omega)_{\eta=0}e^{-l\eta} . \tag{3.12}$$

If at the input of the active medium the detuning parameter is zero, it remains identically zero, everywhere. We define as resonant propagation the situation in which $\Omega = 0$ for all values of η. In this case a closed-form solution exists for the atomic variables R_1, R_2, and R_3 which is easily shown to be (see e.g., Belenov *et al.* in Ref. 3)

$$R_1 = [R_3^e/(1+\gamma^2)^{1/2}]\sin\sigma ,$$

$$R_2 = [R_3^e/(1+\gamma^2)^{1/2}](\cos\sigma - 1) , \tag{3.13}$$

$$R_3 = [R_3^e/(1+\gamma^2)](\cos\sigma + \gamma^2) ,$$

where R_3^e is the population difference $|c_b|^2 - |c_a|^2$ just prior to the arrival of the leading edge of the pulse at a given depth into the active (or absorbing) medium.

In arriving at Eqs. (3.13) we have assumed implicitly the swept excitation initial conditions

$$R_1(\tau = 0, \eta) = 0 ,$$

$$R_2(\tau = 0, \eta) = 0 , \tag{3.14}$$

$$R_3(\tau = 0, \eta) = R_3^e .$$

The parameter $\sigma(\eta, \tau)$ is related to the Rabi frequency by the simple relation

$$\frac{\partial \sigma(\eta, \tau)}{\partial \tau} = \omega_R \tag{3.15}$$

or by

$$\sigma(\eta, \tau) = \int_0^\tau d\tau^1 \, \omega_R(\eta, \tau^1) . \tag{3.16}$$

Hence, σ is proportional to the integrated pulse energy from the leading edge of the pulse up to a given value τ of the local time. The total pulse energy will be denoted by

$$\Sigma(\eta) = \lim_{\tau \to \infty} \sigma(\eta, \tau) ; \tag{3.17}$$

It is easy to derive the equation of motion for $\sigma(\eta, \tau)$. From the first field equation (3.10) and from Eq. (3.13) we have

$$\frac{\partial^2 \sigma}{\partial \eta \partial \tau} = \frac{g}{(1+\gamma^2)^{1/2}}\sin\sigma \frac{\partial \sigma}{\partial \tau} - l\frac{\partial \sigma}{\partial \tau} . \tag{3.18}$$

We find a major difference between Eq. (3.18) and the "area" equation derived by Arecchi and Bonifacio[9] for a one-photon amplifier. The Arecchi-Bonifacio area equation has the form

$$\frac{\partial^2 \sigma}{\partial \eta \partial \tau} = G\sin\sigma - l\frac{\partial \sigma}{\partial \tau} , \tag{3.19}$$

where σ represents the area under the electric field envelope. In our case the nonlinear driving term on the right-hand side of Eq. (3.18) contains the product $\sin\sigma(\partial\sigma/\partial\tau)$. This circumstance allows us to make general statements concerning the behavior of the pulse energy which are drastically different from those derived for a one-photon amplifier.

In order to analyze the spatial variation of the pulse energy, we integrate Eq. (3.18) with respect to the local time τ. Upon taking the limit $\tau \to \infty$, we have

$$\frac{\partial}{\partial \eta}\Sigma(\eta) = -l\Sigma(\eta) + \frac{g}{(1+\gamma^2)^{1/2}}[1 - \cos\Sigma(\eta)] . \tag{3.20}$$

The solution of Eq. (3.20) in the lossless case ($l = 0$) is found to be

$$\Sigma(\eta) = 2 \operatorname{arc\,cotan}\left(\operatorname{cotan}\tfrac{1}{2}\Sigma(0) - \frac{g}{(1+\gamma^2)^{1/2}}\eta\right) + 2k\pi \tag{3.21a}$$

or

$$\Sigma(\eta) = 2 \operatorname{arc\,cotan}\left(\operatorname{cotan}\tfrac{1}{2}\Sigma(0) - \frac{g}{(1+\gamma^2)^{1/2}}\eta\right) + 2(k+1)\pi \tag{3.21b}$$

where (3.21a) applies when the expression in large parentheses is positive, and (3.21b) when it is ne-

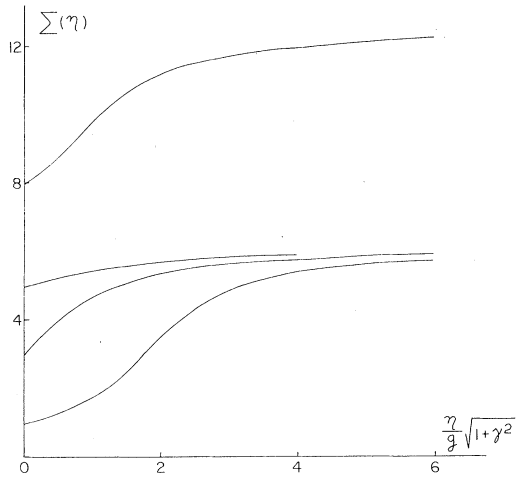

FIG. 2. Spatial behavior of the pulse energy $\sum(\eta)$ (Eqs. (3.21a) and (3.21b)] for different values of the input value $\sum(0)$.

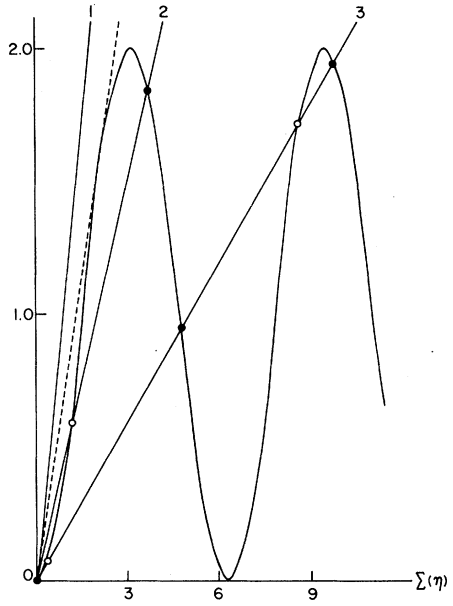

FIG. 3. Asymptotic steady-state solutions of the area equation [Eq. (3.20)] correspond to the intercepts of the straight lines $(1+\gamma^2)^{1/2}(l/g)\sum(\eta)$ with the curve $1-\cos\sum(\eta)$. The straight lines 1, 2, and 3 have slopes equal to 1, $\frac{1}{2}$, and $\frac{1}{5}$, respectively. The stable solutions are marked with solid circles. The unstable solutions are marked with open circles. The critical slope (dashed line) is 0.7246.

gative. The integer number k equals the integral part of $\Sigma(0)/2\pi$, and $\Sigma(0)$ is proportional to the input pulse energy.

Typical solutions are shown in Fig. 2 corresponding to different input energies $\Sigma(0)$. It is obvious both from Eq. (3.20) and from the solutions in Fig. 2 that the efficiency of the amplifier, measured for example in terms of the initial rate of growth, is not a monotonic function of the input energy, as in the case of an ordinary amplifier. The initial rate of growth, instead is maximum for $\Sigma(0)=\pi$ and odd multiples of π, while it vanishes for $\Sigma(0)=2\pi, 4\pi$, etc. In the latter case the pulse energy is conserved during the propagation.

Detailed information about the pulse envelope cannot be obtained from Eq. (3.20). A computer simulation of Eqs. (3.8) and (3.10) has shown that, even when the pulse energy is conserved during the evolution, pulse reshaping takes place with a continuous narrowing of the pulse and a subsequent growth of the peak power.

Interesting predictions can be made also about the asymptotic behavior ($\eta \to \infty$) of a pulse even when the field losses are taken into account ($l \neq 0$). In this case the asymptotic solution $\Sigma(\infty)$ must satisfy the transcendental equation

$$1-\cos\Sigma(\infty)=(1+\gamma^2)^{1/2}(l/g)\Sigma(\infty)\,. \qquad (3.22)$$

It is apparent that multiple steady-state solutions are possible. Three typical situations are indicated in Fig. 3. With reference to this figure, the straight line labeled 1 corresponds to $(1+\gamma^2)^{1/2}l/g=1$. The only solution of Eq. (3.22) in this case is $\Sigma(\infty)=0$. The pulse is completely dissipated by the scattering losses and no energy or power simplification is possible in the inverted medium. The straight line labeled 2 corresponds to $(1+\gamma^2)^{1/2}l/g=\frac{1}{2}$. It intersects the curve $1-\cos\Sigma(\infty)$ in three points. It is trivial to verify from Eq. (3.20) that the intercepts marked with solid circles represent possible stable solutions, whereas the intercept marked with an open circle is an unstable asymptotic solution. In the case of the straight line labeled 3, we have chosen $(1+\gamma^2)^{1/2}l/g=\frac{1}{5}$. Three possible stable solutions exist [one corresponding to the trivial case $\Sigma(\infty)=0$].

Several conclusions can be gathered from the above observations.

(i) Two simultaneous requirements must be satisfied for the asymptotic propagation of a pulse with an energy $\Sigma(\infty)\neq 0$. First, the parameter $(1+\gamma^2)^{1/2}\times l/g$ must be smaller than the absolute critical value 0.7246. (The slope of the dashed line in Fig. 2.) Secondly, the incident pulse energy must be larger than the value of Σ corresponding to the first unstable root for a given choice of $(1+\gamma^2)^{1/2}l/g$. If both conditions are satisfied, the total pulse energy will converge to a stable nonvanishing value.

(ii) The output of the pulse energy can be larger or smaller than its input value $\Sigma(0)$ depending on the magnitude of $\Sigma(0)$ relative to the nearest stable solution $\Sigma(\infty)$. This aspect of the propagation prob-

lem will be confirmed by our computer simulations where it is seen that power amplification in the coherent regime can occur both with energy amplification or reduction.

(iii) There is no small signal gain; i.e., even if the parameter $(1+\gamma^2)^{1/2}l/g$ is sufficiently small an input signal with energy smaller than the first unstable root will not be amplified.

(iv) It is anticipated that whenever multiple stable solutions are possible, the nth stable root $\Sigma(\infty)$ corresponds to a pulse envelope that has been split into $n-1$ distinct pulses (see Fig. 6).

In addition to the above remarks, we can add that the field equations (3.10) do not allow a steady-state solution for the pulse envelope. This feature is confirmed by our computer simulations where it is seen that, when the threshold conditions are satisfied, the peak power continues to grow and the pulse duration becomes smaller and smaller, as the pulse energy approaches its stable asymptotic value.

IV. COMPUTER SIMULATION STUDIES

The coupled set of equations (3.8) and (3.10) has been analyzed with a hybrid computer in the limiting case of resonant interaction and with the atomic system prepared in a swept excitation mode corresponding to the initial conditions (3.4), and to the boundary conditions

$$\Omega(\eta=0,\tau)=0 \quad \omega_R(\eta=0,\tau)=\omega_R(\tau)\,. \tag{4.1}$$

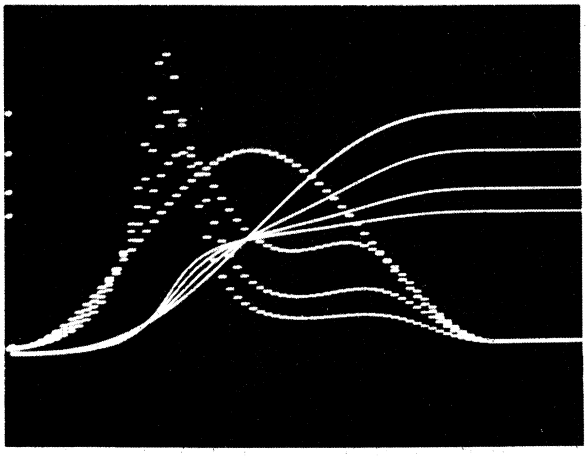

FIG. 4. Computer simulation illustrating the evolution of the pulse intensity through the amplifying medium. The different dashed curves represent the intensity envelope in different sections of the amplifier. The solid curves are the corresponding integrated energy $\sigma(\eta;\tau)$. The value of $\sigma(\eta,\tau)$ at the far right gives the total energy $\sum(\eta)$. The horizontal axis is the local time axis with $\tau=0$ (leading edge of the pulse) at the far left. The input energy is $\sum(0)=8$ and the gain-to-loss ratio $g/l(1+\gamma^2)^{1/2}=2$. Note the transient envelope modulation.

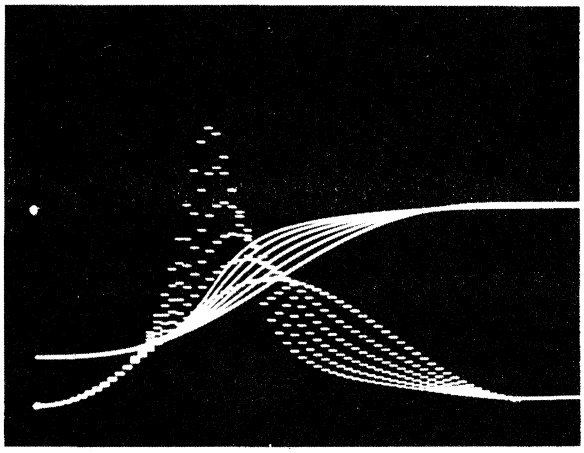

FIG. 5. Evolution of a pulse with an initial energy very close to the expected asymptotic stable value. The input energy is $\sum(0)=5$ and the gain-to-loss ratio is 5.

The input pulse envelope has the form

$$\omega_R(\tau)=\omega_R^0\sin^2(\pi\tau/\tau_p)\,, \tag{4.2}$$

where τ_p denotes the pulse duration from the leading to the trailing edge.

As expected the detuning parameter Ω remains identically equal to zero throughout the evolution of the pulse, an indication that the computer round-off error has been kept small. An additional check of the accuracy of the solution is provided by the conserved nature of the linear combination of atomic variables $R_2-\gamma R_3$ as one can verify at once from Eq. (3.8) in the resonant case. We have monitored $R_2-\gamma R_3$, and found it to be essentially constant over the entire range of integration of the problem.

Figures 4–6 show some typical solutions of the

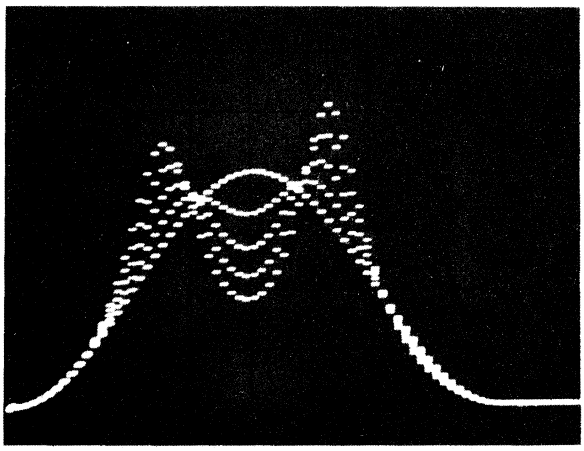

FIG. 6. Pulse splitting and double pulse propagation in the coherent limit. The input area is $\sum(0)=9.8$ and the gain-to-loss ratio is 5.

propagation problem. The dotted lines represent successive pulse shapes at various sections along the amplifier, while the solid lines give the corresponding pulse energies $\sigma(\eta,\tau)$. As shown in Sec. III the input energy $\Sigma(0)$ and the gain-to-loss ratio $g/l(1+\gamma^2)^{1/2}$ control the asymptotic behavior of the pulse energy under coherent propagation conditions. In Fig. 4 the gain to loss ratio equals 2. As shown in Fig. 3, only one steady-state value of $\Sigma(\infty)$ is possible corresponding to the present choice of $g/l(1+\gamma^2)^{1/2}$ provided $\Sigma(0)$ exceeds its threshold value. This behavior is confirmed by the solution shown in Fig. 4. In addition, the initial energy $\Sigma(0)$ is larger than the predicted asymptotic value for the chosen gain to loss ratio. As a result the pulse energy decreases monotonically as the pulse envelope reshapes itself.

In Fig. 5, we display the evolution of a pulse with an initial energy $\Sigma(0)=5$ propagating in a medium with a gain-to-loss ratio equal to 5. In this case two steady-state values of $\Sigma(\infty)$ are possible. Corresponding to the chosen initial value of $\Sigma(0)$, the solution evolves into a single narrow pulse with an asymptotic energy that can be read off directly from Fig. 3.

In Fig. 6, we show the effect of increasing the incident pulse energy while keeping the gain-to-loss ratio equal to 5, as in the previous case. The envelope reshapes into two separate pulses which appear to evolve more or less independently.

Additional solutions obtained for larger values of the gain-to-loss ratio have confirmed that the nth stable energy $\Sigma(\infty)$ corresponds to a pulse envelope that has split into $n-1$ separate pulses.

Further work to incorporate the effects of detuning and irreversible atomic relaxation is in progress.

ACKNOWLEDGMENTS

One of us (L.M.N.) wishes to express his appreciation to Professor Rodolfo Bonifacio for a very informative conversation. The support and encouragement of the Quantum Physics, Physical Sciences Directorate at Redstone Arsenal, Alabama, and especially of R. A. Shates and Dr. C. M. Bowden, is gratefully acknowledged.

---

*Work partially supported by the Army Research Office Grant No. DAAG29-76-G-0075 and by the ONR Contract No. NOO14-76-C-1082.

[1]A. M. Prokhorov, Science 149, 828 (1965).

[2]P. P. Sorokin, N.Braslau, IBM J. Res. Dev. 8, 177 (1964).

[3]S. R. Hartmann, IEEE J. Quant. Electron. QE-4, 802 (1968); E. M. Belenov and I. A. Poluektov, Sov. Phys.-JETP 29, 754 (1969); M. Takatsuji, Physica (Utr.) 51, 265 (1971); Phys. Rev. B 2, 340 (1970); D. Grischkowski, Phys. Rev. Lett. 24, 866 (1970); N. Tan-no, K. Yokoto, and H. Inaba, Phys. Rev. Lett. 29, 1211 (1972).

[4]For a critical comparison of the different theoretical approaches see, for example, D. Grischkowski, in *Laser Applications to Optics and Spectroscopy, Vol. II of Physics of Quantum Electronics Series*, edited by S. F. Jacobs, M. Sargent, III, J. F. Scott, and M. O. Scully (Addison-Wesley, Reading, Mass., 1975).

[5]N. Tan-no, K. Yokoto, and H. Inaba, J. Phys. B 8, 339 (1975); 8, 349 (1975); M. Takatsuji, Phys. Rev. A 11, 619 (1975); D. Grischowsky, M. M. T. Loy, and P. F. Liao, *ibid.* 12, 2514 (1975); R. Brewer and E. L. Hahn, *ibid.* 11, 1641 (1975).

[6]R. L. Shoemaker and R. G. Brewer, Phys. Rev. Lett. 28, 1430 (1972); N. Tan-no. K. Yokoto, and H. Inaba, *ibid.* 19, 1211 (1972); H. Nakatsuka, J. Okada, and M. Matsuoka, J. Phys. Soc. Jpn. 37, 1406 (1974).

[7]L. E. Estes, L. M. Narducci, and B. Shammas, Nuovo Cimento Lett. 1, 175 (1971).

[8]R. L. Carman, Phys. Rev. A 12, 1048 (1974).

[9]F. T. Arecchi and R. Bonifacio, IEEE J. Quant. Electr. QE-1, 169 (1965).

[10]S. L. McCall and E. L. Hahn, Phys. Rev. Lett. 18, 1019 (1967).

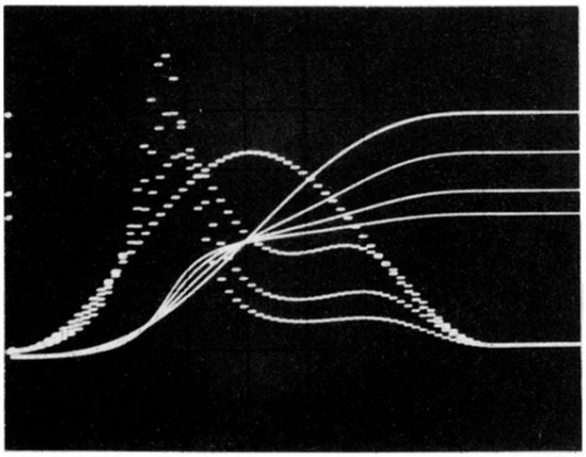

FIG. 4. Computer simulation illustrating the evolution of the pulse intensity through the amplifying medium. The different dashed curves represent the intensity envelope in different sections of the amplifier. The solid curves are the corresponding integrated energy $\sigma(\eta:\tau)$. The value of $\sigma(\eta,\tau)$ at the far right gives the total energy $\sum(\eta)$. The horizontal axis is the local time axis with $\tau=0$ (leading edge of the pulse) at the far left. The input energy is $\sum(0)=8$ and the gain-to-loss ratio $g/l(1+\gamma^2)^{1/2}=2$. Note the transient envelope modulation.

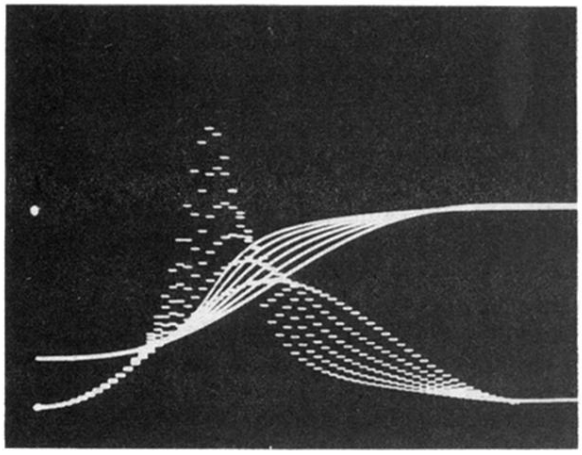

FIG. 5. Evolution of a pulse with an initial energy very close to the expected asymptotic stable value. The input energy is $\sum(0) = 5$ and the gain-to-loss ratio is 5.

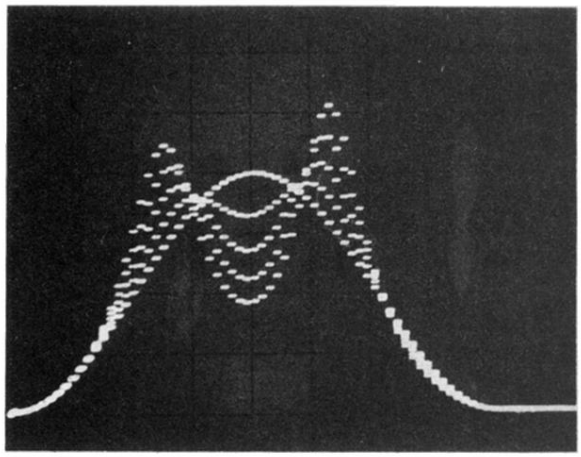

FIG. 6. Pulse splitting and double pulse propagation in the coherent limit. The input area is $\sum(0) = 9.8$ and the gain-to-loss ratio is 5.